The final publication is available at

http://doi.org/10.1177/1468087416636281

Additional Information

On the Rate of Injection Modelling applied to Direct Injection Compression Ignition Engines

Raul Payri; Jaime Gimeno; Ricardo Novella; Gabriela Bracho
CMT Motores Térmicos, Universitat Politecnica de Valencia

Abstract

Modern engine design has challenging requirements towards maximum power output, fuel consumption and emissions. For engine combustion development programs, the injection system has to be able to operate reliable under a variety of operating conditions. Today's legislations for quieter and cleaner engines require multiple injection strategies, where it is important to understand the behavior of the system and to measure the effect of one injection on subsequent injections. This study presents a methodology for 0D modeling the mass flow rate and the rail pressure of a common rail system, constructed from a set of experimental measurements in engine-like operating conditions, for single and multiple injection strategies. The model is based in mathematical expressions and correlations that can simulate the mass flow rate obtained with the Bosch tube experiment, focusing on the shape and the injected mass, using few inputs: rail pressure, back pressure, energizing time, etc. The model target is to satisfy two conditions: lowest computational cost and to reproduce the realistic injected quantity. Also, the influence of the rail pressure level on the start of injection is determined, especially for multiple injection strategies on the rate shape and injected mass. Good accuracy was obtained in the simulations. Results showed that the model error is within the 5%, which corresponds at the same time to the natural error of the injector and to the accuracy of the measures which had been done. The benefits of the model are that simulations can be performed quickly and easily for any operation points, and on the other hand that the model can be used in real-time on the engine test bench for mass estimations when doing additional experiments or calibration activities.

1. Introduction

Currently, most of engine optimization works revolve around several parameters and one of them is the fuel injection characteristics. Usually, the injection strategy determines the achievement of the emission targets or the engine efficiency ([1,2]). Due to the flexibility of the common rail injection system, a huge variety of strategies can be employed, going from the traditional single injection event to the most sophisticated pilot-main-post multi-injection cases, where the diversity of possibilities involves the injection duration and the separation between them, with further consequences on the combustion-emission performance.

The engine performance improvement is being possible due to the implementation of different analysis techniques. On one hand, the understanding of the physics underlying Diesel engines among combustion diagnosis models, which are based on the instantaneous in-cylinder pressure (usually referred to as thermodynamic models) through the determination of the rate of heat released (RoHR) ([3],[4],[5]). On the other hand, extended

analysis are carried out by combining direct engine testing with 0D, 1D or 3D-CFD modeling to relate the trends followed by pollutant emissions with the in-cylinder local conditions ([6], [7],[8]). In all those techniques one of the important inputs are the injected mass and/or the shape of the injection event [9,10,11].

Frequently the rate of injection ROI is obtained from experimental sources ([12],[13],[14]), and if the ROI measurements are very accurate, the diagnosis tools and the CFD models are expected to provide proper solutions. Nevertheless, considering the numerous injection configurations that can be tested in those analyses for reaching the target engine points, the ROI testing matrix could be extremely large. An alternative to reduce the experimental matrix or to complement the ROI data base is to develop a model of the injection shape. The large number of technical reports regarding the modeling of the dynamic behavior of the injection system confirms this ([15],[16],[17]). In one hand, the ROI modelling using 1D tools is based on the characterization of all the components of the fuel injection system (injector, pump, valves) etc, which implies to know and understand in detail all the geometries and physical phenomena in the elements. Besides, the 0D model assumes the injection system as a black box and focuses on modeling the response of the signal as a function of certain input parameters, using adequate mathematical expressions, providing analogous versatility of the 1D model with less geometrical information.

The main purpose of the current work is to develop a 0D model able to estimate the shape of the rate of injection and the injected mass quantity in engine-like operating conditions, using as a reference the rail pressure signal, for single and multiple injection strategies. Specifically, the methodology is composed by two approaches: the first one is focused on estimating the injection rate itself by an empirical formulation based on experimental data collected at the injection test rig; the second one is focused on the simulation of rail pressure dynamics along the injection process. Also, to determine the influence of the rail pressure level on the start of injection, especially for multiple injection strategies on the rate shape and injected mass.

This paper is structured in five sections. First, the fluid-dynamics equations that are used for describing the injection process are presented, which are based on the hydraulic flow characterization. In the second section, the experimental facilities and the methodology are described, explaining the mass flow test rig, the injection system and the engine test bench. Third, the methodology for developing the model is presented. Afterwards, the validation is carried on by comparing the mass flow rate provided by the model with those obtained experimentally by means of a mass standard injection rate based on Bosch method.

2. Experimental tools

2.1. Injection Rate test rig

The mass flow rate of injection was measured using commercial long-tube equipment. This device measures the chronological sequence of an individual fuel injection event. The measuring principle used is the Bosch method [12, 13] which consists of a fuel injector that injects into a fuel filled measuring tube. The back pressure is provided with a cavity filled with nitrogen, which avoids back pressure oscillations. With the purpose of determining the total mass injected, a gravimetric balance is placed downstream of the rate of injection meter as is explained in detail in [13] and depicted in Figure 1.
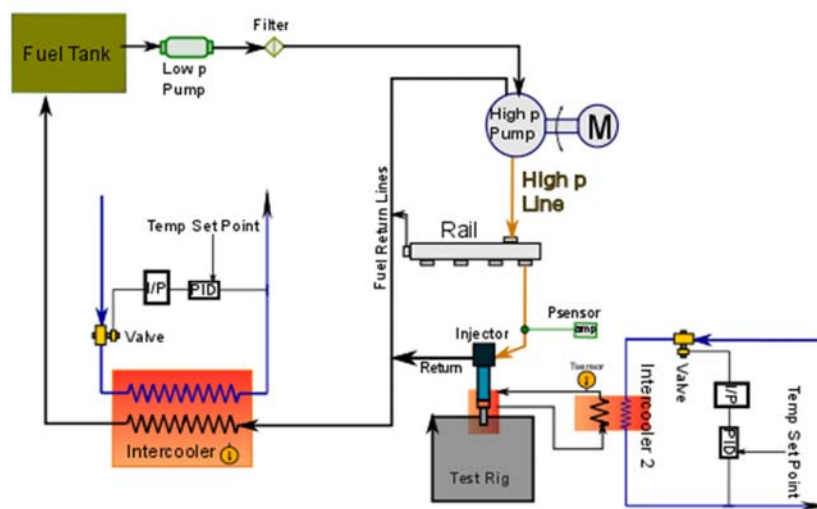

Figure 1. Sketch of the injection rate test rig

Fifty repetitive measurements were carried out at the same test point (energizing time, rail pressure and backpressure). The rate of injection signal is corrected using the gravimetric balance value, where the measurement error for these tests is generally around 0.5% with proper calibration of the equipment, being lower for long injections.

2.2. Injection System and test conditions

To carry out this work a state of the art Common-Rail injection system is used. The system is constituted by a high pressure pump and a conventional accumulator with a pressure regulator, which allows fuel injections up to 200 MPa and relatively constant pressure. The injector unit is a commercial Delphi 1.5. The characteristics of the nozzle are shown in Table 1.

Table 1. Nozzle characteristics.

Nozzle Type	Microsac
Number of Spray holes	8
Outlet hole diameter, Do (µm)	90
Spray Cone Angle (º)	155

The injector holder temperature was maintained at a constant temperature of 70ºC for all experimental test conditions (and all experimental devices). The study has been done using commercial diesel with a density of 838.3 kg/m^3 (at 15ºC) and kinematic viscosity of 2.44 mm^2/s (at 40ºC).

For the hydraulic characterization of the nozzle different injection conditions were tested, covering the operating range of the injector. The rail pressure was varied between 23 MPa and 200 MPa. The duration of energizing the injector was varied from 250 (representative of pilot injections) to 1500 µs, which is long enough to ensure that the needle position is at maximum lift, being the flow mainly controlled by the nozzle holes. The measurements were performed by systematicly increasing the injection pressure and the energizing time. The authors did not notice any hysteresis in the testing campaign used for the main model; however, when the injectors were extensively used in the engine the maximum and the duration of the ROI changed as is presented later on in the Appendix section. The experimental matrix carried out is summarized in Table 2.

Table 2. List of operating range tested in the ROI device.

Name	Unit	Tested Values
Rail Pressure	MPa	23 / 40 / 80 /100 / 120 / 160/ 180 / 200
Back Pressure	MPa	2.4 / 5.0 / 8.0
Energizing Time	µs	250 / 275 / 300 / 400 / 500 / 600 / 700 / 900 / 1100 / 1300 / 1500
Number of cycles per test condition	-	50

3. Methodology

For this study, a simplified 0D model that reproduces the rate of injection has been developed. The model is based in mathematical expressions and correlations that can simulate the mass flow rate obtained with the Bosch tube experiment, focusing on the shape and the injected mass, using few inputs: rail pressure, back pressure, energizing time, etc. The model should satisfy two conditions: lowest computational cost and to reproduce the realistic injected quantity. The potential benefits of the model are that simulations can be performed quickly and easily for any operation points (even if they were not measured), and on the other hand that the model can be used in real-time on the engine test bench for mass estimations when doing additional experiments or calibration activities.

The procedure consisted on:

1. To perform mass flow rate measurements for a wide test matrix (covering the complete operational range of the injection system), varying all significant parameters, such as rail pressure, back pressure and energizing time. The testing conditions are indicated in Table 2.
2. An analysis of the signal is done for selecting the more appropriated mathematical expressions that could suit the injection shape. Different alternatives can be considered depending on each case, for example straight slopes, first and second order system response, exponential, polynomial, Bezier curves, etc.
3. To adjust the model expressions, finding the best fitting with all the measured conditions and then modelling each equation coefficient as a function of input parameters. Depending on the rate of injection shape and the characteristics of the parameter influence, initial poor correlations could be obtained at first; therefore, this step needs an iterative process, with some false steps in between, until the form of the equations and the coefficients obtained satisfied the required or are representative for all the conditions.
   Moreover, at this step of the study the authors evaluated the possibility of having tuning constants for each pressure to best fit the data; nevertheless, this possibility was discarded in order to avoid discontinuities and to have a general equation that fits all the operating range (although this condition makes more challenging the modelling and the iteration process), obtaining a general coefficient set that works for all the injection pressures and back pressures at the same time.

3.1. Rate of Injection Modelling

The first step is to evaluate the experimental rate of injection shape. Figure 2 shows a general silhouette of the rate of injection signal for short (left side) and long injections (right side), where each curve is the ensemble average of the 50 cycles measured. It can be seen that the long injections have the particularity to maintain the same shape for almost any condition. For whatever input parameter, the main injections have a trapezoidal shape,

while the pilots have a triangular one. Then, the simplest procedure is to make a segmentation of these forms and associate them with mathematical expressions.
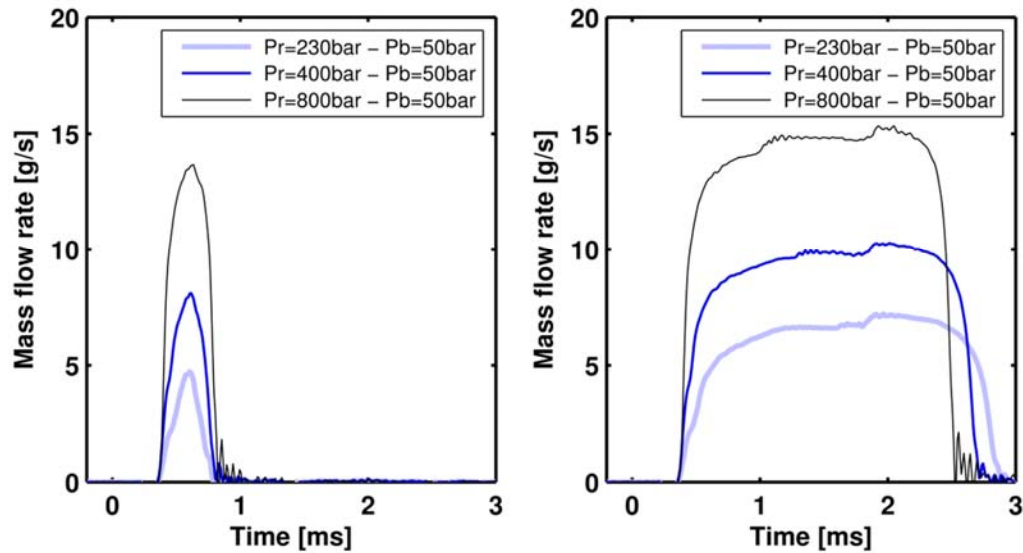

Figure 2. Experimental Rate of Injection. Left side: pilot injections (ET 250 us); right side: main injections (ET 1500us)

1) Single injection decomposition:

Figure 3 depicts a standard mass flow rate measurement shape. The signal is converted in parametric equations in two parts: Wave expression at stationary conditions and a shape function.
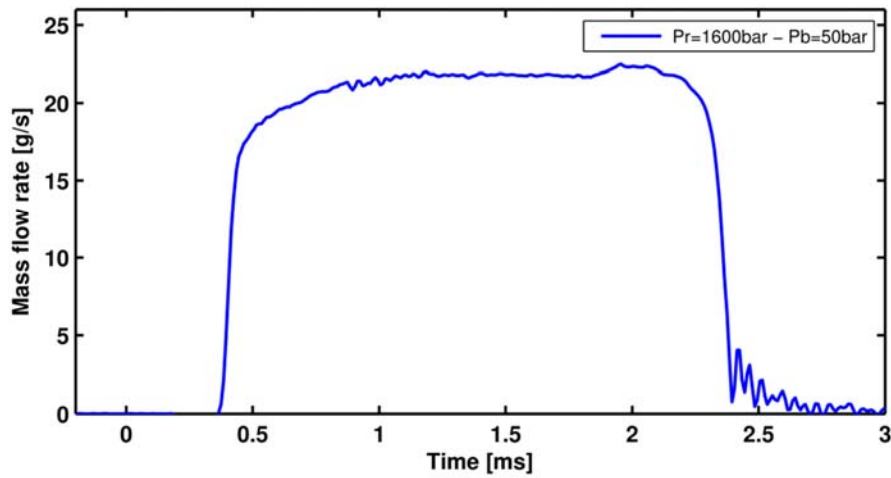
Figure 3. Rate of Injection signal

The wave expression model is based on second order behavior as indicate Equations (1) and (2), where $\bar{m}$ is the averaged mass flow rate and $W(t)$ is the wave function itself, which is the most common expression for representing the step-response of a damped system.

$$y = \bar{m} \cdot W(t) \qquad \textbf{(1)}$$

$$W(t) = A \cdot exp(-\gamma \cdot t) \cdot sin(\omega \cdot t - \phi) + ... \qquad \textbf{(2)}$$

The coefficients of the wave function are adjusted to the experimental data using non-linear fittings. Then the shape function $S(t)$ is obtained in Equation (3) dividing the real mas flow rate signal by $\overline{m}\,W(t)$, obtaining a non-dimensional curve that is more robust for doing the further parametrization.

$$S(t) = \frac{\dot{m}(t)}{\bar{m} \cdot W(t)} \qquad \textbf{(3)}$$

The left side of Figure 4 depicts the experimental rate of injection signal in blue and the corresponding wave function in green continuous line. The result of operating Equations (1), (2) and (3) is represented in right side of Figure 4. The shape signal is a trapezoid with softened corners.
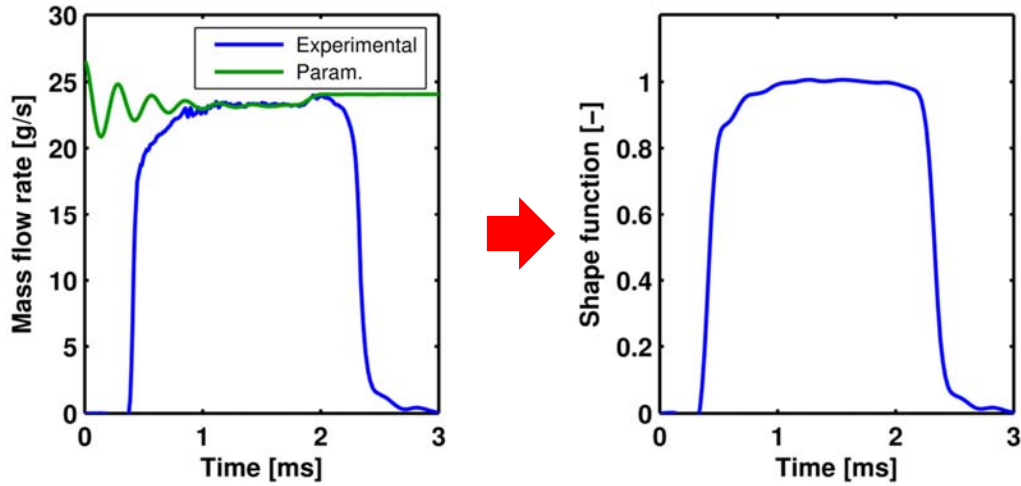
Figure 4.Real Rate of Injection signal, wave function and shape function

Figure 5 depicts the decomposition of the shape signal. The trapezoid is defined using the simplest mathematical expressions that can be used providing the best accuracy. The functions selected for the model were straight slopes (for opening and closing phases), and second order Bezier curves to soften the corners (delimited by Cs_x, Cs_y, Ce_x and Ce_y). Finally, 8 parameters (plotted on Figure 5) are defined that should be parametrized: SOI, Duration of Injection, start slope, end slope and four control points which describe the Bezier curves.
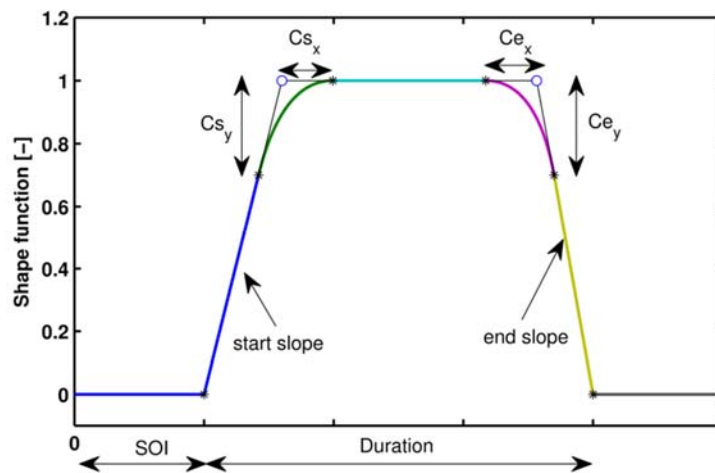

Figure 5.Shape function segmentation

2) Variable dependency:

The next step is to adjust each extracted parameters as a function of input parameters such as the rail pressure, back pressure, actuation time, etc.

The stationary mass flow $\overline{m}$ is reached when the needle lift does not constrain anymore the flow and it will depend on the velocity of the flow at the hole exit. Then, it is characterized combining Bernoulli's equation and mass conservation equation [18]. Mass conservation leads to Equation (4) where $\overline{m}$ is the mass flow rate, ρ_f represents the liquid density, A_o is the geometrical cross section of all the orifices, the u_B is the Bernoulli's theoretical velocity which can be represented as a function of the rail pressure and back pressure as Equation (5).

$$ \dot{m}_f = C_d \cdot A_o \cdot \rho_f \cdot u_B \qquad \textbf{(4)} $$

$$ u_B = \sqrt{\frac{2(P_r - P_b)}{\rho_f}} \qquad \textbf{(5)} $$

Combining Equations (4) and (5), and since the geometric area is constant, the mass flow parametrization can be written as a function of the pressure drop, as in Equation (6)

$$ \dot{m}_f = Cm_1 + Cm_2\sqrt{\rho_f} + Cm_3\sqrt{P_r - P_b} \qquad \textbf{(6)} $$

The coefficients Cm_1 to Cm_3 are adjusted to the experimental data (using linear fittings), minimizing the relative error and a statistical number which uses the interval of the normal distribution. In Figure 6 the results from the experimental hydraulic characterization of the nozzle is depicted. In that figure, the flow rate is represented against the square root of the pressure drop for all the rail pressure and back pressure tested. As it can be seen from the figure, mass flow rate increases linearly with the square root of the pressure drop, which is expected since it is a non-cavitating nozzle.

Regarding the opening and closing slopes (α and β respectively), they depend on the velocity of the needle movement. Since the needle movement is commanded by force equilibrium, is expected that the most significant parameters that have an influence on the opening slope are the pressure levels at both sides of the injector. Additionally, the force equilibrium that controls the needle movement depends on several variables, such as the actuating element type (solenoid or piezoelectric), the control area (area pressurized by the fluid in the control volume), the effective area of the control valve, and the inertial mass of the system [19,20]. For the current work, unfortunately the inner geometry of the injector is unknown, therefore the opening and closing slopes are represented by rail and back

pressures levels, and the other parameters should be represented as fitting coefficients. The determination of the expressions for these particular parameters was challenging, as was mentioned in Section 3, since some iteration went into selecting the most appropriate functions and coefficients. After the iterative process, Equations (7) and (8) represent the best polynomial expression that fit the opening (α) and closing (β) slopes respectively. The comparison of the fitting curve against the experimental data is shown in Figure 7.
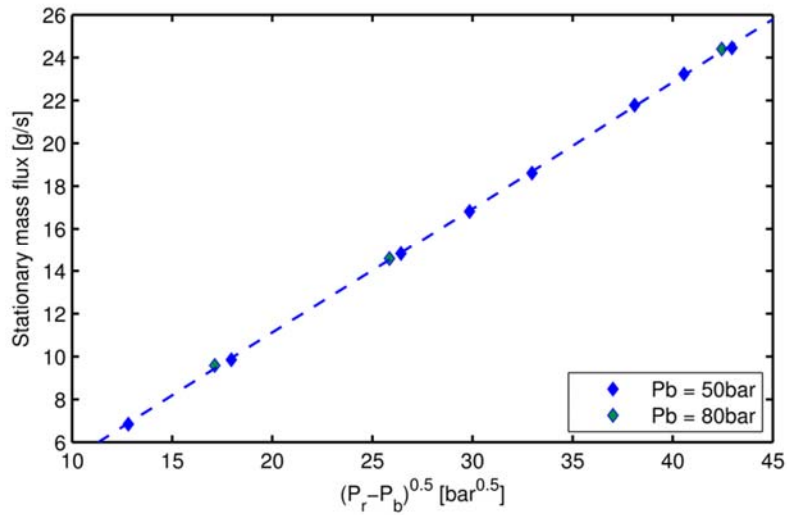

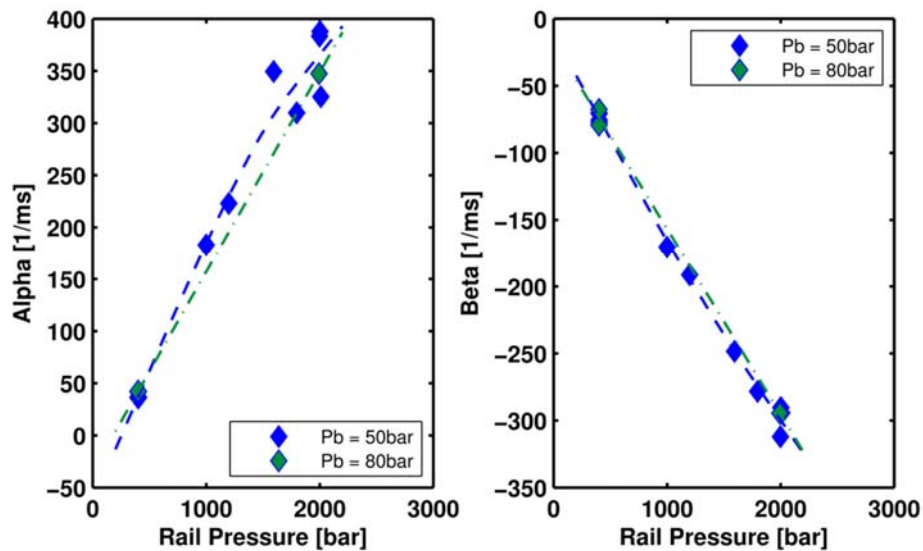Figure 6. Mass flow against square root of pressure drop. Experimental data and fitted curve

Figure 7. Experimental data and fitted curve. a) Opening slope as a function of Rail pressure and back pressure. b) Closing slope as a function of Rail pressure and back pressure

$$\alpha = C_{\alpha 1} + C_{\alpha 2}\sqrt{P_r - P_b} + C_{\alpha 3}P_b + C_{\alpha 4}P_r + C_{\alpha 5}P_r^{2} + C_{\alpha 6}P_r\sqrt{P_r - P_b} \qquad (7)$$

$$\beta = C_{\beta 1} + C_{\beta 2}\sqrt{P_r - P_b} + C_{\beta 3}P_b + C_{\beta 4}P_r + C_{\beta 5}P_r^{2} \qquad (8)$$

One of the parameters that is important for the engine testers and combustion modelers is the hydraulic delay or start of injection (SOI) which is defined as the time difference between the start of the electrical pulse and the exact moment when the fuel starts to flow from the nozzle to the combustion chamber. The SOI itself is not going to change the mass flow rate shape; however it will determine the initial point of the curve. The understanding of this parameter is necessary for the injection time location in the engine map as well as in the 1D or 3D computations. It is also a parameter to take into account in multiple injections strategies for determining the proper separation between consecutive injections (dwell time). For the studied injector technology, the physical variable that influences the most the SOI is the rail pressure, since the greater the rail pressure the higher is the force on the needle, and so the needle lifts faster [20,21]. The back pressure has also an influence as it helps the needle to lift too. An additional term to take into account is the flow velocity in the injector sac, which is also a function of the pressure as was described previously; therefore the SOI can be parametrized as a function of pressures as shown in Equation (9). In Figure 8, the correlation for the SOI as a function of pressures obtained from the experimental data has also been represented.

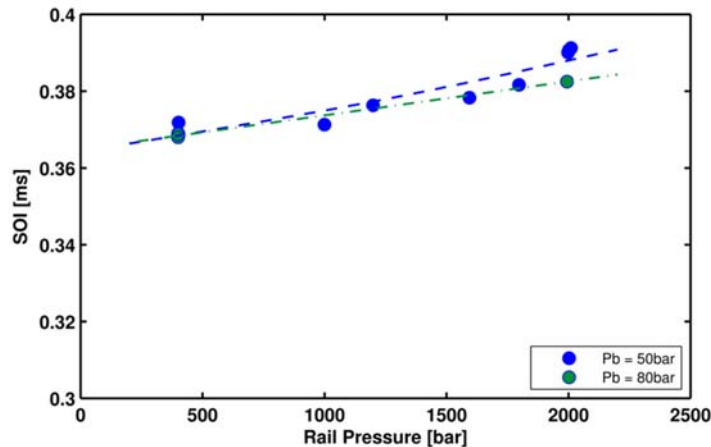$$SOI = Cs_1 + Cs_2\sqrt{P_r - P_b} + Cs_3P_b + Cs_4P_r + Cs_4P_r^{2} \qquad (9)$$

Figure 8. SOI against rail pressure. Experimental data (●) and fitted curve (--)

Finally, one of the most difficult parameters to model is the Duration of Injection (DOI) as several variables affect it. Indeed, the injection duration depends on the electrical pulse, on the electrical valve configuration, as well as on the time lapse taken by the pressure in the control volume to recover the rail pressure as soon as the electric component is not energized anymore. Due to the inertia of the injector, usually the injection duration is longer than the solenoid excitation time; therefore, for multi-injection strategies the end of the injection should be taken into account in order to configure the next injection [20].

In order to simplify the characterization of this parameter, a time variable is defined as the time between the end of the injection and the beginning of the pulse, isolating the influence of the hydraulic delay. In this way, the influence of the energizing time (ET) is shown in Figure 9. It can be seen that there are two slopes related to the lift of the electric component and the lift of the needle. For small electrical pulses, the electric component moves short distance, and when the electric component stops the energizing, the time to close the control valve is smaller. On the other hand, when the electrical pulse is short, the closing occurs before reaching the maximum needle lift position, it will close faster and the DOI will be shorter. Of course, other geometric characteristics of the inner control volumes will impact the DOI, but due to the internal unknowns they were not considered for the parametrization. The best fitting to characterize the injection duration is shown in the Equation (10).
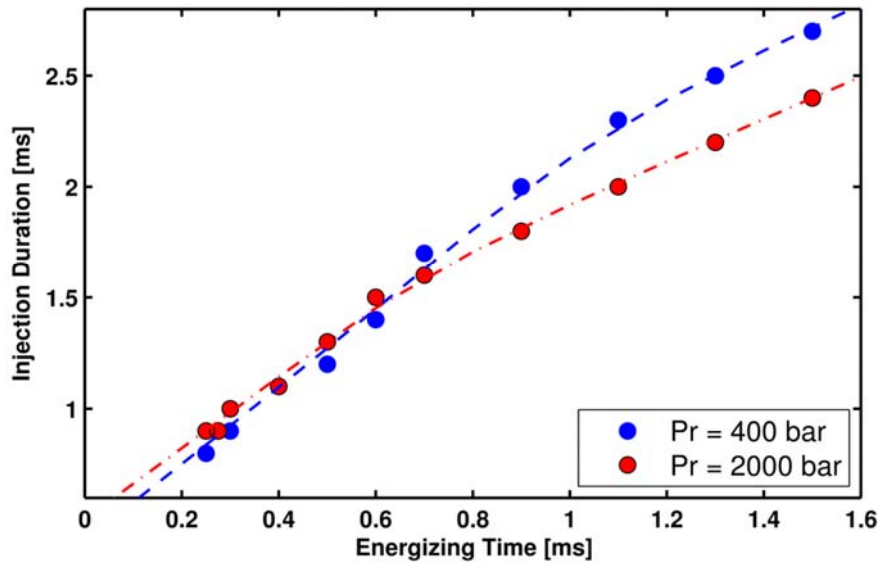
Figure 9. Injection duration vs. the energizing time

$$ID = C_{ID1} + C_{ID2}\sqrt{P_r - P_b} + C_{ID3}P_b + C_{ID4}P_r + C_{ID5}P_r^2 + C_{ID6}\sqrt{P_r - P_b}\,P_r + C_{ID7}ET - SOI \quad \textbf{(10)}$$

On the other hand, in this injector type the mass flow rate suddenly increases when the energizing pulse finishes. This can be associated to the control volume pressure dynamics when the electrical signal is over, that will also decrease/stop the return flow delivering all the fuel quantity towards the nozzle exit. This increase can be modelled as a logistic function, where the x-value of the Sigmoid's midpoint is characterized as t_{rise} in Equation (11).

$$t_{rise} = C_{R1} + C_{R2}ET \quad \textbf{(11)}$$

Once all the coefficients are parametrized and the wave $W(t)$ and shape $S(t)$ functions are determined, the rate of injection $\dot{m}(t)$ is computed using Equation (12), where the stationary mass flux depends mainly on the rail pressure and the back pressure; the wave function depends mainly on the rail pressure and the shape function depends on the pressures and energizing duration.

$$\dot{m}(t) = \overline{m} \cdot W(t) \cdot S(t) \quad \textbf{(12)}$$

3.2. Multi-Injection

The injection process characterization in modern engines should be able to deal with many injections per stroke as necessary. The modeling of multi injection is based on single-injection equations presented above plus the dwell time definition. In this particular case the Dwell Time (DT) is referred to the time difference between the start of energizing of the subsequent injection (SOE_{i+1}) and the end of energizing of previous one (EOI_i), as shown in Equation (13) and Figure 10.

$$DT_E = SOE_{i+1} - EOE_i \qquad \textbf{(13)}$$

Usually the DT_E is an input from the engine software, therefore the SOE_{i+1} can be determined, being the local reference for the start of injection SOI_{i+1} which is obtained then with Equation (9). Similarly, the other coefficients and parameters for the wave and shape functions are determined using the same inputs values than the ones of the precedent injection event.
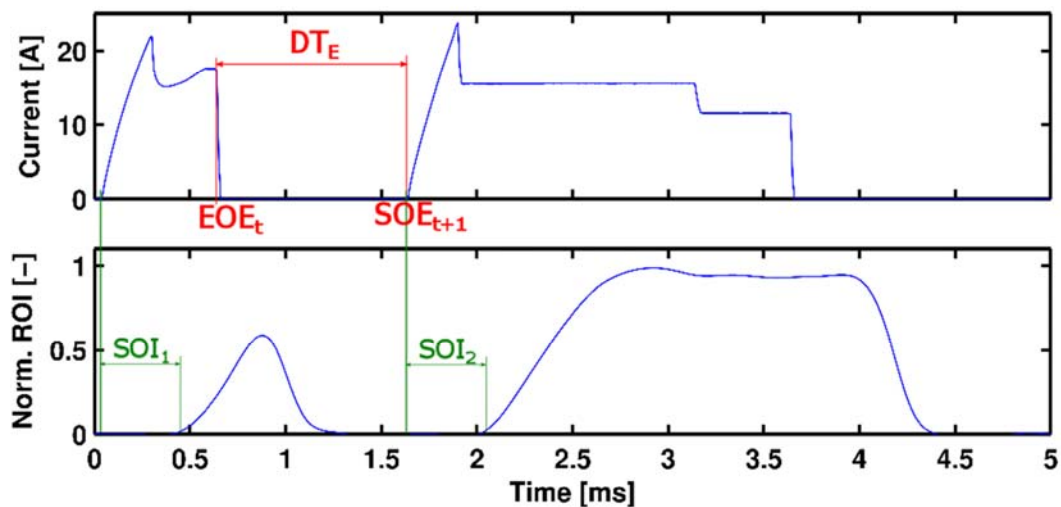

Figure 10. Multi - injection dwell time definition

The limit of the model is the prediction of injection shape when two subsequent injections are overlapped as the dwell time between them is very short. For these situations additional characterization is required and will be implemented for future studies.

3.3.Rail pressure Modelling

Figure 11 shows a real pressure signal in the rail during an injection event. It can be seen a pressure drop when the injection occurs due to the fuel delivery into the combustion chamber and some waves or oscillations are present while the pressure control acts and recovers the stabilized level. However, if the fuel delivery strategy is a multi-injection one, other injections are done before this recovering time. Sometimes, depending on the injection pressure level, the pressure drop in the rail could descend around 8-12 MPa which is representative for the ROI shape (as seen previously, the opening slope and the maximum values depends on the pressure), therefore the inputs for modelling the consecutive injections should be readjusted.
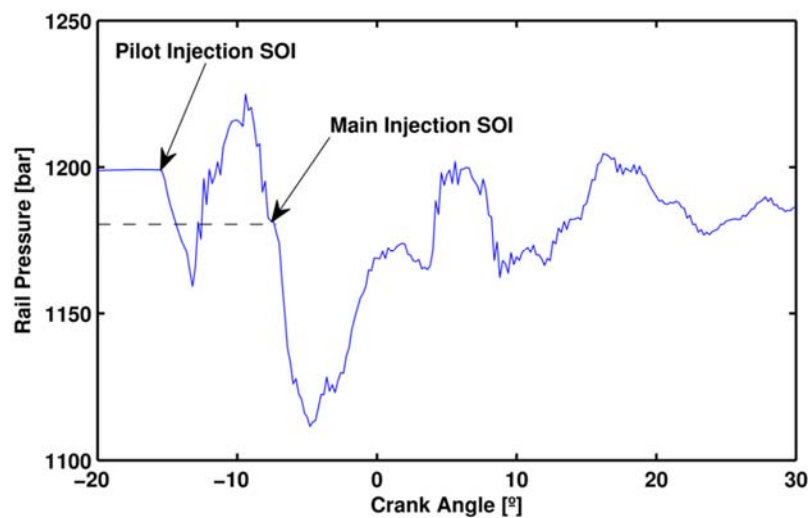

Figure 11. Rail pressure signal during an injection event

The study of the pressure into the common rail is a complex matter due to all the elements involved in the system. After several considerations based on the wave period time and the studied time [22, 23], the most convenient is to create a simplified 1D model for representing the physical problem. Figure 12 shows the elements considered for the pressure model, from the pump to the injector, where the system is considered as an assembly of three constant volumes and a fuel line between the rail and the injector.
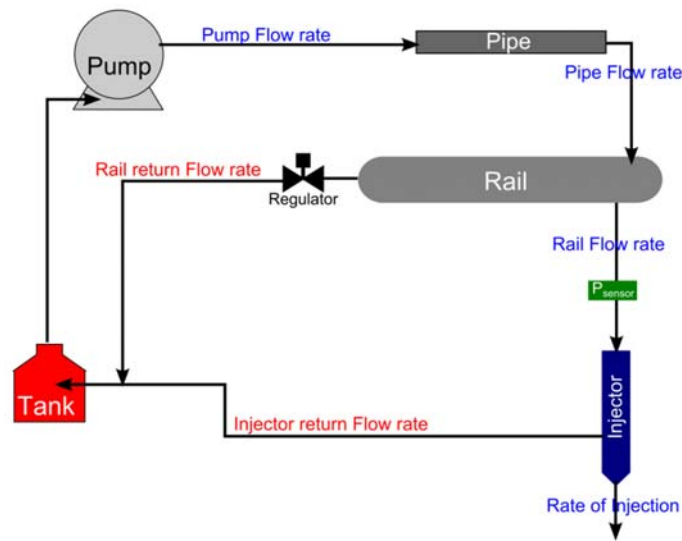
Figure 12. Scheme of the common rail components

The geometric data were measured in the laboratory, except the injector volume. The pump system is a high pressure radial piston pump Bosch-CP3 and its volumetric flow rate will be considered as constant through the time; for instance, the oscillations due to the architecture of the pump are neglected. The control of the rail pressure regulator is done with a PID controller and it will be considered as a first order system. The volumetric flow of the regulator $Q_{regulator}$ is described in Equation (14), where the coefficient k_r is adjusted measuring in laboratory the response time of the system for a step-input between two pressures.

$$Q_{regulator} = k_r(P_r - P_{regulator}) + Q_{pump} \quad (14)$$

For the constant volumes, the model of fluid compressibility is used in order to characterize the difference of pressure as a function of the different volumetric flow rates. As a first approach, the tube between the pump and the rail is considered as a constant volume, which absorbs the pressure waves enough to avoid the discretization as in the rail-injector line. The different flow rates for the constant volumes have to be characterized for each step of time in order to solve the compressibility model. The fuel line between the rail and the injector has to be discretized in one dimension in order to model the wave effects which are significant. The pressure sensor is located in this fuel line, at 100 mm from the injector.

To close the model, the injection and the injector return flow are the most significant since they cause the pressure drop in the common rail system. The volumetric flow rate of injection is directly the output from the ROI model described in previous section divided by the fluid density. The return flow is modeled from the injection rate (since they use to have the same behavior) [24], adjusting the maximum level.

The governing equations for solving the system at each operating point through space and time are the Euler equations of continuity and momentum. The Euler equations are resolved

thanks to the Godunov scheme and the HLL solver of the Riemann problem. Since the pressure levels are very high, the fluid is not considered as incompressible anymore, then for the different constant volumes the modulus of compressibility is required in order to know the pressure depending on the flow rates. The Bulk modulus is directly linked to the fluid density and speed of sound [23,25], which are characterized with the pressure and temperature as referred in [26], and is obtained using the Equation (15).

$$B = \rho_f c^2 \qquad (15)$$

Bernoulli equation and flow rate definition are used to compute the internal flow rates, indicated in Equations (16), (17) and (18):

$$Q_{rail} = u_1 A_{line} \qquad (16)$$

$$Q_{injector} = u_{end} A_{line} \qquad (17)$$

$$Q_{pipe} = A_{pipe} \sqrt{\frac{2(P_{pipe} - P_{rail})}{\rho_{pipe}}} \qquad (18)$$

The final step is to define the boundaries and the initial conditions. The conditions at the beginning in terms of pressure, density and null velocity are assumed to be uniform for the entire domain in the model. The boundary conditions are calculated for each time step, using the method of the fictitious points for finding the intercell flux with the HLL solver (see Figure 13). The transmissive boundary involves that the fictitious point is equal to the nearest point (Equations (19) to (20)).
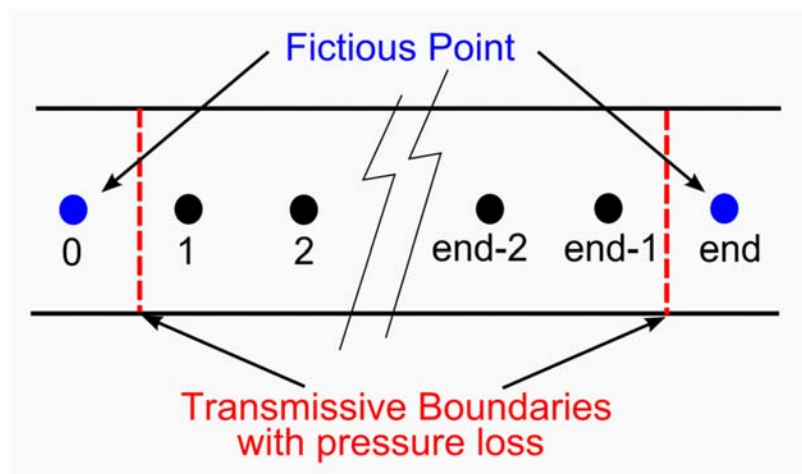

Figure 13. Scheme of the Boundary conditions

$$u_o = u_1 \quad ; \quad u_{end} = u_{end-1} \tag{19}$$

$$P_o = P_1 + u_o \cdot C_{Lo} \frac{\rho_1 u_o^2}{2} \quad ; \quad P_{end} = P_{end-1} + u_{end} \cdot C_{Lend} \frac{\rho_{end} u_{end}^2}{2} \tag{20}$$

$$\rho_o = \rho(P_o, T); \quad \rho_{end} = \rho(P_{end}, T) \tag{21}$$

Once the pressure in the rail is determined, the mass flow rate for multi-injection can be re-estimated using the instantaneous pressure level as an input parameter.

4. Validation

4.1. Mass flow rate modelling

In order to verify the model, several experimental measurements were performed using the injection rate test bench previously described. In Figure 14, the experimental mass flow rates are compared with those obtained from the model for two injection pressure levels and several energizing times. In Figure 15, the total amount of fuel mass of the model, calculated as the integral of the ROI curve, and the experimental total mass are also compared for the two rail pressure levels: 23 and 160 MPa, which are representative for all the operating range behavior.

Overall, both figures show the ability of the model to predict the experimental results with quite high level of accuracy both in terms of rate of injection shape and total injected mass, where the maximum deviations found are lower than 8% (for pilot injections and cases where the ET is used as input). When the injected mass is used as an input the deviation is lower. There is a test point at 23 MPa that over estimates the DOI for the third case, despite good agreement elsewhere. That particular point is located in the region of operation where there is a change in the slope that describes the injected mass vs. ET function; this change in trend is a standard behavior in this injector type, related to the transition between the "triangle shape" ROI (where the needle throttling plays an important role), and "trapezoid shape" ROI (where the flow rate is dominated by the nozzle discharge coefficient) [14,15].

The measurements have provided a well characterized injector thanks to measurements over a wide range of conditions. However, one limitation of the model is that the modeling constants chosen are not universal; therefore, its implementation outside the measured ranges or for other nozzle geometries should be executed carefully.
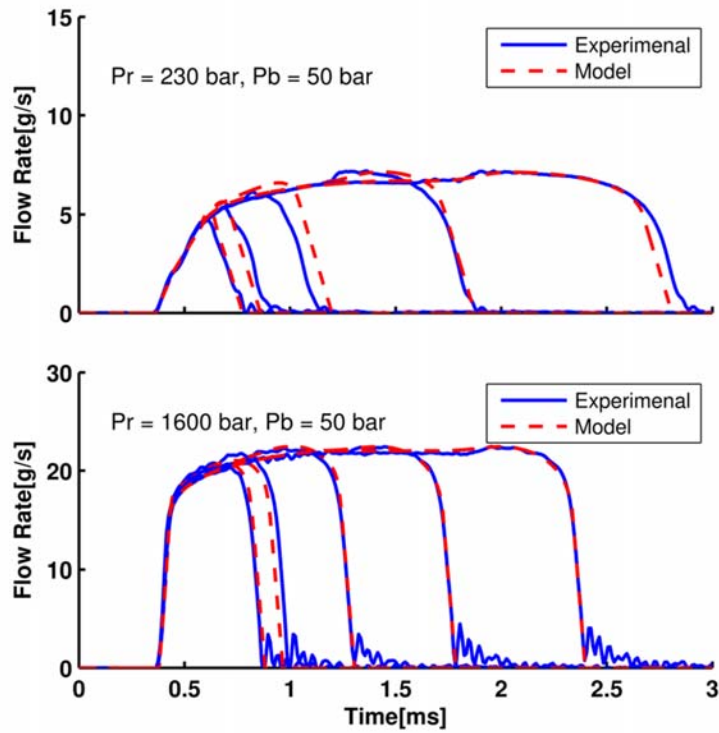
Figure 14. Model validation at different injection pressures and different energizing times
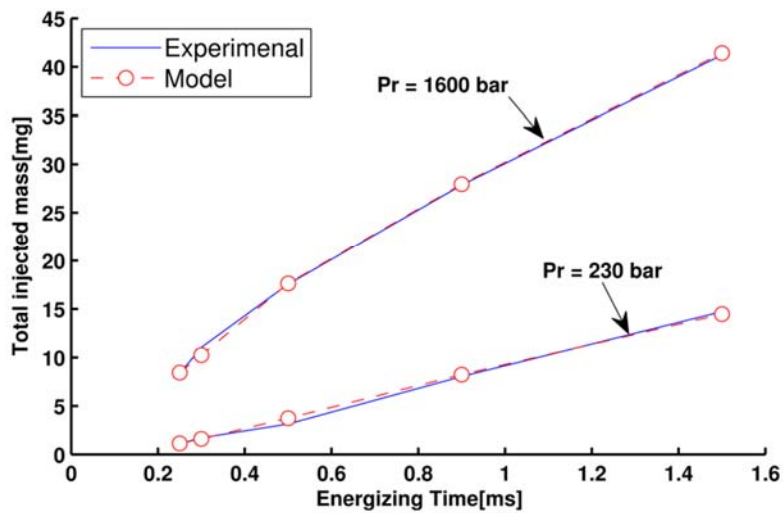

Figure 15. Experimental injected mass and model injected mass comparison

4.2. Validation of rail pressure modelling

The comparison between the pressure model and the experimental data is shown in the left side of Figure 16. The pressure trace of the main injection is shown in the upper part, while the pressure curve for a pilot injection is depicted in the bottom part. The pressure signal from the 'modeling' results is being recorded from a point representative of the physical distance of 100 mm. This distance should be indicated correctly since the comparison is sensitive to the sensor location in terms of wave phasing; if the sensor is considered farthest to the injector the pressure wave estimation might be somehow delayed (taking into account the ratio with the speed of sound, the fuel line length and the time-event of the injection the deviation, the deviation could be considerable).

In Figure 16 it can be seen that the model reproduces satisfactorily the pressure drop as well as the water hammer effect in both cases, short and long injections. The frequency of the oscillations fits very well with the experimental data too. However, in the majority of the cases the second minimum is overestimated, the inaccuracy at this particular zone during the injection event is due to the lack of knowledge of the return flow which has been approximated.

On the other hand, the right side of Figure 16 shows the relative error between the model and the experiments as a function of time. In all the cases modelled the relative error is below 5 % providing good accuracy.
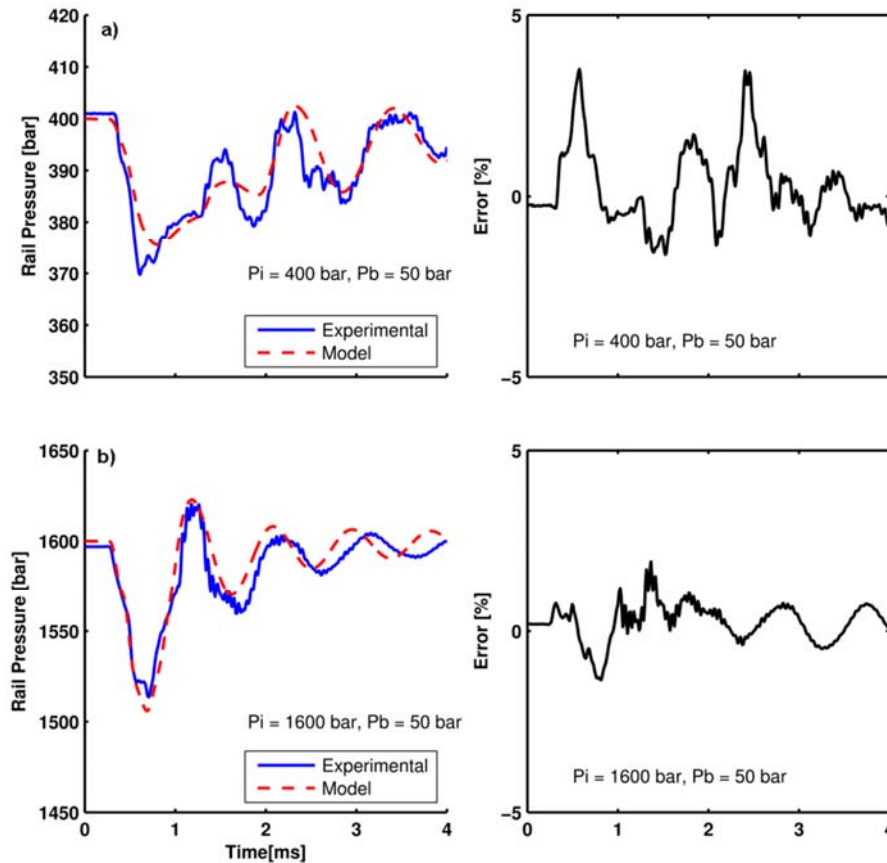
Figure 16. Left side: Comparison of the pressure model and the experimental data (a) Low rail pressure (400 bar) & Long Injection (900us), (b) High rail pressure (1600 bar) & short injection (300us). Right side: Relative error of the model as a function of the time for (a) and (b).

4.3. Implementation to multi-injection modelling

As previously stated, when more than one injection per cycle occurs, size and shape of the subsequent injections are influenced by the first injection. Any size of injection produces a pressure wave in the injection pipe which can affect the injection occurring afterwards, as showed Figure 11. Also, moving the separation between pilots and main injections causes the main injection to start at different pressure level, varying the opening, maximum and closing slopes, resulting in variations in injection quantity. To reproduce this phenomenon, the proposed approach combines the pressure wave model and the ROI model, using the instantaneous pressure as the input value at the start of each subsequent injection event.

In order to demonstrate the usefulness of the combined model implementation, two different simulations are carried out, the first one considering the pressure as constant, and the second simulation taking into account the pressure waves in the system produced by the first injection.

A multi-injection process is modeled with three injections which represent the pre-injection for the noise, the main injection for the power and the post-injection for the pollutants; the particular input parameters are: constant rail pressure of 165 MPa, energizing time 0.250, 1.200, 0.270 ms respectively and the dwell time values are 0.5 and 1.5 ms. The result is depicted   in
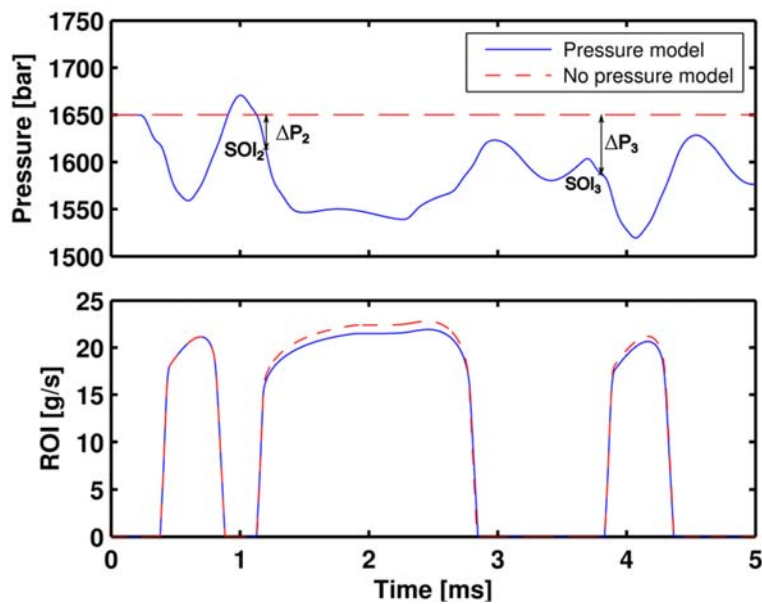

Figure 17 with the dashed red line. The second simulation is performed modeling simultaneously the rail pressure waves and the mass flow rate of the three injections (with the instantaneous pressure value at the start on injection), for the same energizing times.

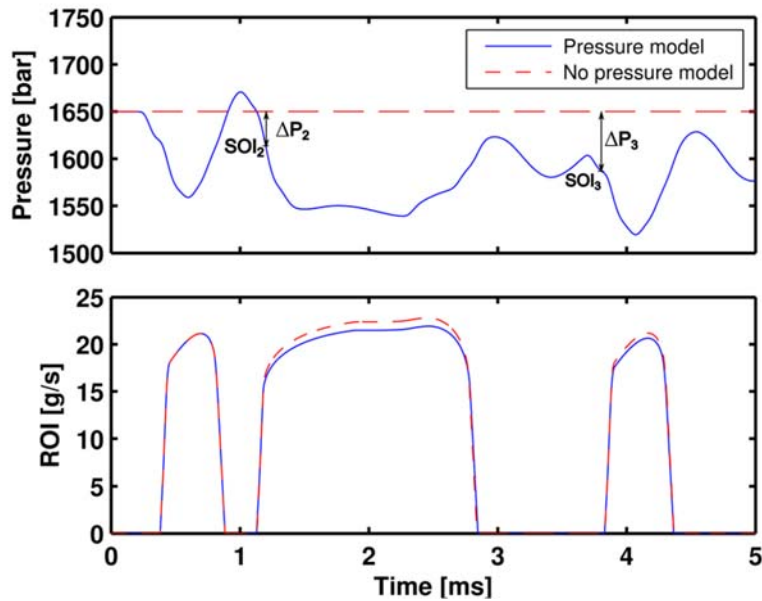The   outcome   is   depicted   in

Figure 17 in blue continuous line. It can be seen how the rail pressure drops and the typical waves of the system reduce the instantaneous pressure at the beginning of the second and third injections, decreasing slightly the opening slope and the ROI in stabilized conditions (as was demonstrated before in in previous sections), reducing the injected mass quantity.

As seen in the figure, if the rail pressure remains constant during the multi-injection process, the total mass injected will have an overestimation of 3.21%. The improved estimation of the flow rate brings a sufficient reason to do the modeling of the pressure in the common rail system in order to reduce the errors at the most.
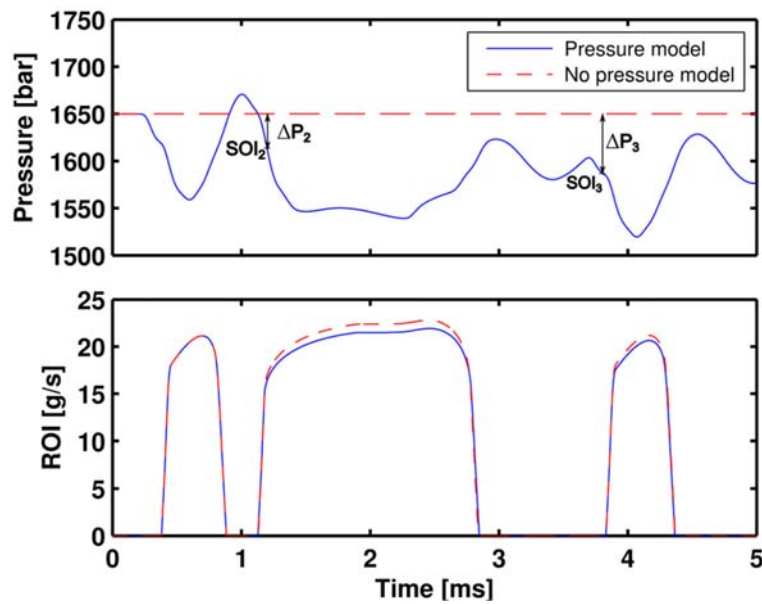
Figure 17. Multi-injection modelling: constant rail pressure and modeled rail pressure. Pr = 1650bar; Pb = 50 bar, ET1 = 250us; ET2 = 1200us; ET3 = 270us.

4.4. *Implementation in the Engine*

One of the targets of the ROI model developed in this study was its implementation in the engine development process, as a baseline for the estimation of the injected mass directly in the test bench while doing the testing, and, in the other hand, in the definition of the boundary conditions for further CFD analysis or combustion diagnosis.

In order to assess the accuracy of the model and the operation of the approach, the injection system modelled was installed in a state of the art engine test bench and several tests were carried out. Two variables were evaluated in the validation at the engine operation: the shape of the rail pressure signal and the total injected mass.

4.4.1. Engine architecture and test cell characteristics

Experimental activities were performed in the single-cylinder research version of an innovative Renault engine concept, consisting of a two-cylinder DOHC 2-stroke HSDI CI engine with scavenge loop, which is currently under development.

The combustion chamber has four poppet valves with double-overhead camshafts and a staggered roof geometry, specifically designed for masking the flow of air between the intake and exhaust valves, allowing proper scavenging of the burnt gases while keeping short-circuit losses as low as possible during 2-stroke operation. The definition of the engine architecture, boost system requirements, combustion chamber geometry and

scavenging characteristics of this newly designed engine were reported in previous publications [27, 28].

A hydraulic cam-driven Variable Valve Timing system allows delaying intake and exhaust valve timings with a cam phasing authority of +30 degrees from base timing, as it was detailed in a previous investigation [29, 7]. In this research, the key valve timing angles (EVO/EVC/IVO/IVC) were defined at those crank angle degrees (CAD) where the given valve lift was 0.3 mm. The single cylinder research version of the Renault 2-stroke engine concept has been manufactured by Danielson. As a reference,

Table 3 lists detailed engine specifications.

Table 3. Main engine specifications.

Engine type	2-stroke compression ignition
Displacement	365 cm3 (single cylinder)
Bore × Stroke	76 mm × 80.5 mm
Connecting Rod Length	133.75 mm
Compression ratio	17.6:1
Number of Valves	4 (2 intake & 2 exhaust)
Type of scavenge	Poppet valves with scavenge
Valvetrain	DOHC with VVA
Nominal intake valve timing (set at VVT=0)	IVO=161.9 CAD aTDC IVC=251.6 CAD aTDC
Nominal exhaust valve timing (set at VVT=0)	EVO=122.6 CAD aTDC EVC=226.9 CAD aTDC
Fuel injection system	Diesel common rail HSDI

The single-cylinder engine operates with a conventional diesel piston providing a geometric compression ratio equal to 17.6 and wide angle injector nozzle. The injector unit is the same employed in the rate of injection test rig, equipped with a 8 holes nozzle, with hole diameter of 90 µm and a spray cone angle of 155º.

The single-cylinder engine test cell is equipped with independent water and oil cooling circuits, an external compressor unit with its dryer for providing water-free compressed air to simulate the required boosting conditions, and an additional low pressure EGR circuit to provide arbitrary levels of cooled EGR even at high intake pressures. The fuel consumption of the engine is measured with an accuracy of 0.2% using a gravimetric dynamic fuel meter. Measurements of O_2, CO, CO_2, HC, NO_X, N_2O, and EGR rate are performed for all the tests with a state-of-the-art HORIBA 7100 DEGR gas analyzer. Soot emissions traced by the filter smoke number (FSN) are measured with an AVL 415 Smokemeter. The instantaneous injection pressure is measured using a piezoelectric sensor installed in the high pressure fuel line, between the rail and the injector, and its signal is sampled with a resolution of 0.2 CAD.

The laboratory setup as well as the required instrumentation and the accuracy of most important measurement equipment, were fully described in previous publications [7,29], in Figure 18 the fuel injection system set-up in the engine is shown.
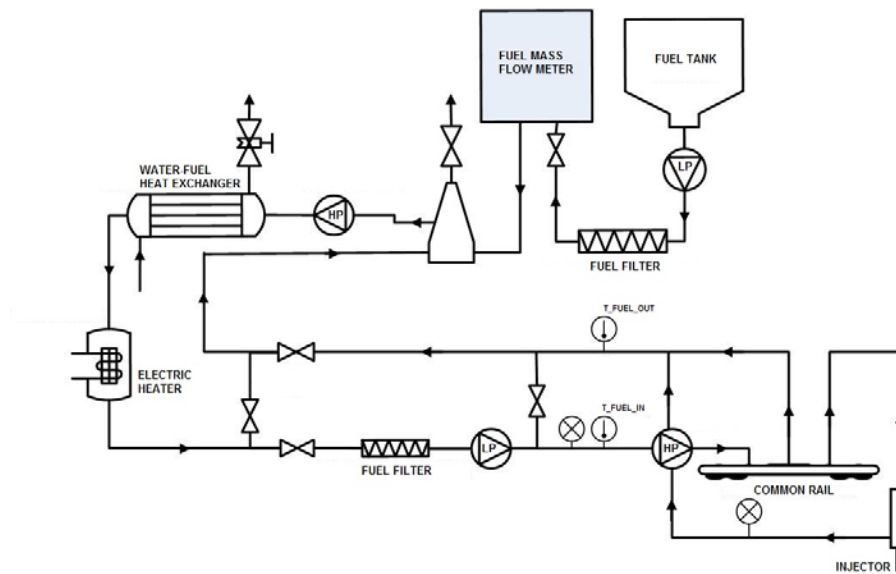
Figure 18. Fuel Injection system set-up in the engine test cell

4.4.2. ROI Validation in the engine

The measurements in the engine-like conditions were performed in the test bench described in section 4.4.1. The injection system (from rail to the injector) is the same than the tested in the ROI test bench, while the fuel lines from the pump to the rail are of a different length, therefore this volumes has to be re-estimated for the pressure model. The tests have been done with the same injector (Table 1) with diesel and gasoline. The interest in using this engine is that it works with advanced combustion approaches (i.e. partially premixed combustion), where the injection process is based on multiple or pulsed injection strategies (so the multiple-injection model can be validated), that should also be accurate in the injection timing in order to have stable combustion and acceptable pollutant performance.

For the engine validation, the three models developed were implemented simultaneously (mass flow rate, pressure model and the used injector correlation explained in the Appendix 1). The used injector correlation was necessary in the rate of injection determination in the engine like conditions because the injector was used for several operating hours.

The ROI and pressure signal were simulated for the experimental point based on a 2 injections strategy, at a rail pressure of 100 MPa, pilot energizing time of 0.240ms and a mass target of 20.5 mg. The results of the rail pressure and the mass flow rate are shown in Figure 19.
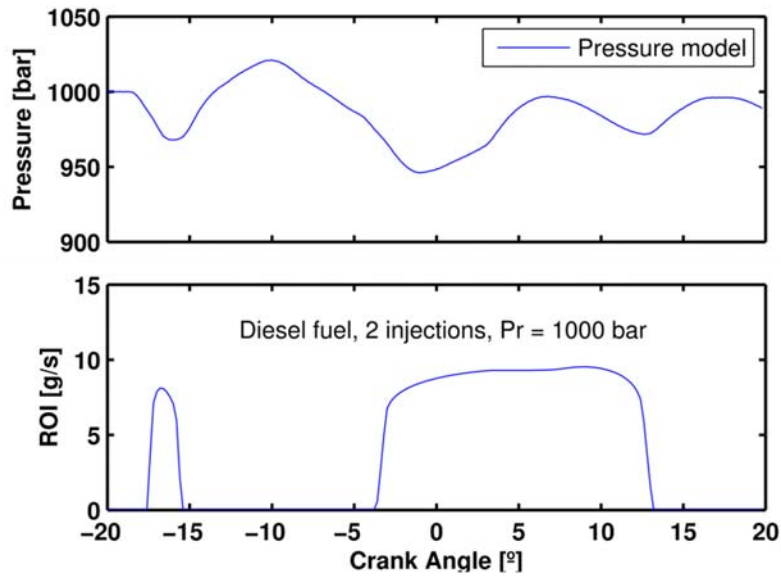
Figure 19. Predicted Injection and pressure with 2-injection strategy

The injected mass calculated with the model is 20.51 mg and the experimental value, measured with the upstream gravimetric balance coupled to the engine, is 20.6 mg which makes an error of -0.46%. The modeled pressure waves are compared against the rail pressure curve from the engine tests, in order to verify that the modeled injection event is in accordance with the experimental data. It can be seen that the modeled ROI is reliable, since there is an interaction between the pressure calculation and the injected mass and ROI model.
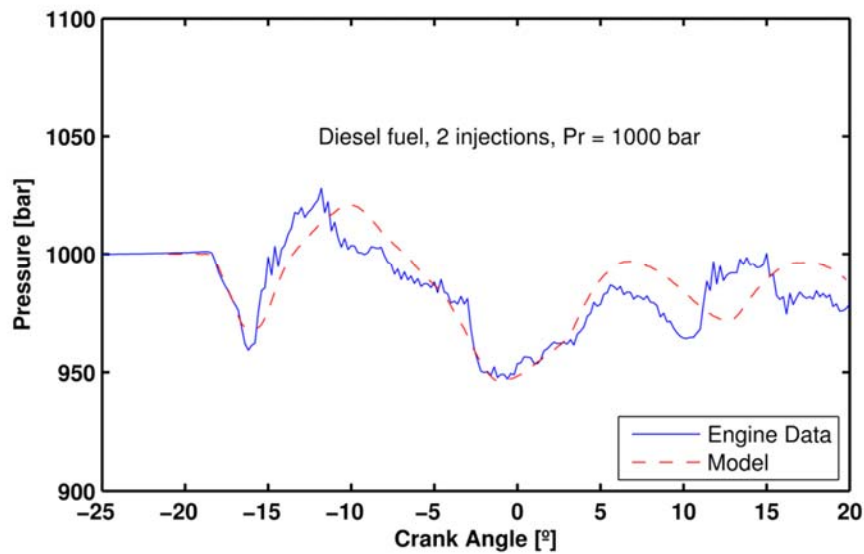
Figure 20. Pressure measured in the engine Rail and modeled pressure comparison with 2-injection strategy

Figure 20 shows the comparison of the pressure measured in the engine rail and the pressure predicted. The results show good agreement of the modeled pressure and the experimental one in terms of pressure drop after pilot injection and main injection (about -13º and -4º respectively), the wave phase and water hammers. For the pressure calculation, the results are quite good regarding to the approximations and assumptions that have been made, especially with the return flow rate.

Moreover, 3-injection strategy test point was also validated (where current duration was set as ET1=0.25ms, ET2=0.53ms and ET3=0.25ms). For this case the rail pressure was 85 MPa and the fuel employed was gasoline (in the same injection system configuration). For this particular condition, the fuel properties equations in the model were also adjusted according to the gasoline physical characteristics. Figure 21 shows the comparison between the rail pressure measured in the engine (black continuous line) and the model results (in dashed red line). The Pressure signal comparison indicates a good agreement in the wave shape, and a good prediction in the pressure level at the start of injection of each injection event (SoI1, SoI2 and SoI3). The pressure signal also corroborates that the injected quantity estimated is in a good agreement since the amplitude of the pressure drop caused by the injection is very similar. Finally, the injected mass measured in the test bench was 11 mg and the predicted total injected mass was 11.13 mg (an error of 1.18%).
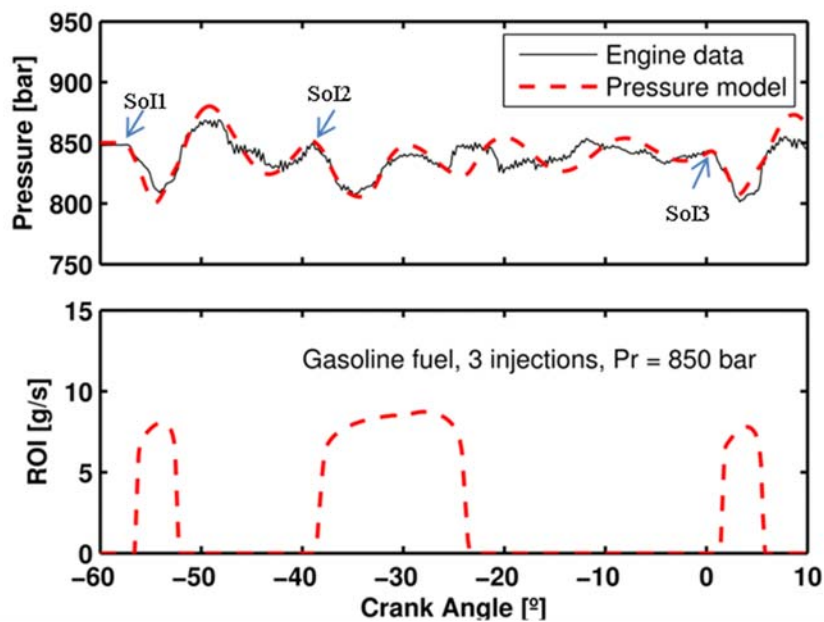
Figure 21. Predicted Injection and pressure with 3-injection strategy Gasoline

5. Summary/Conclusions

This study presents a methodology for modeling the mass flow rate and the rail pressure of a common rail system, constructed from a set of experimental measurements.

The model is based on correlations and quite complex equations, that take into account many variants as mass, duration or energizing time, rail and chamber pressure, etc. The physical characteristics of the injectors were used in order to find suitable equations and so the coefficients for each injector. The measurements over a wide range of conditions have provided a well characterized injector. However, one limitation of the model is that the modeling constants chosen are not universal; therefore, its implementation outside the measured ranges or for other geometry should be executed carefully. It has been noticed that the injection pressure was the parameter which had most impact on the injection model regarding the form and the total injected mass. Besides, the pressure into the common rail system evolves in function of the injection event. It has been seen that the drop of pressure was produced by the fuel which went out from the injector.

For the pressure model, the results are quite good regarding to the approximations that were made especially with the return flow rate. Good accuracy was obtained implementing the models on engine simulations. Results showed that the model error is within the 5%, which corresponds at the same time to the natural error of the injector and to the accuracy of the measures which had been done. Finally, although the model was calibrated for diesel fuel, it was tested in engine-like conditions for gasoline fuel only modifying the return flow and the fluid properties equations, obtaining the same accuracy.

References

1. Fimml, W., Chmela, F.G., Pirker, G., Wimmer,A. Influence of cavitation in the injection nozzle on combustion in diesel engines, International Journal Engine Research, 11, pp. 375-390; 2010.

2. Benajes, J., Novella, R., de Lima, D., Tribotté, P. Analysis of combustion concepts in a newly designed two-stroke high-speed direct injection compression ignition engine. International J of Engine Research, 2014, DOI: 10.1177/1468087414562867.

3. M. Lapuerta, O. Armas, J. J. Hernández, Diagnosis of DI Diesel combustion from in-cylinder pressure signal by estimation of mean thermodynamic properties of the gas, Applied Thermal Engineering 19 (5) (1999) 513-529. doi:10.1016/S1359-4311(98)00075-1.

4. J. Benajes, P. Olmeda, J. Martín, R. Carreño, A new methodology for uncertainties characterization in combustion diagnosis and thermodynamic modelling, Applied Thermal Engineering 71 (2014) 389-399. doi:10.1016/j.applthermaleng.2014.07.010.

5. F. Payri, S. Molina, J. Martín, O. Armas, Influence of measurement errors and estimated parameters on combustion diagnosis, Applied Thermal Engineering 26 (2-3) (2006) 226-236. doi:10.1016/j.applthermaleng.2005.05.006.

6. Benajes, J., García-Oliver, J-M, Novella, R., Kolodziej, C. Increased particle emissions from early fuel injection timing Diesel low temperature combustion, Fuel 94 (2012) 184–190. doi:10.1016/j.fuel.2011.09.014

7. Benajes, J., Novella, R., Martín, J., and De Lima, D., "Analysis of the Load Effect on the Partially Premixed Combustion Concept in a 2-Stroke Hsdi Diesel Engine Fueled with Conventional Gasoline," SAE Technical Paper 2014-01-1291, 2014, doi: 10.4271/2014-01-1291.

8. Musculus, M.P.B., Miles, P.C. and Pickett, L.M. Conceptual models for partially premixed low-temperature diesel combustion. Prog Energ Combust Vol. 39, pp. 246–283, 2013.

9. Naber, J.D., Siebers, D.L., Effects of gas density and vaporization on penetration and dispersion of diesel sprays. SAE Transactions 105(3):82-111,1996, doi: 10.4271/960034.

10. Abraham, J., Pickett, L.M., Computed and measured fuel vapor distribution in a diesel spray. Atomization and sprays. 20:241-250,2010.

11. Som, S., D'Errico, G., Longman, D., Lucchini, T., Comparison and Standardization of numerical approaches for the prediction of Non-Reacting and reacting diesel sprays. SAE Technical paper 2012-01-1263, 2012, doi: 10.4271/2012-01-1263.

12. Bosch W. The fuel rate indicator: a new instrument for display of the characteristic of individual injection. SAE Paper 660749; 1966.

13. Payri R, Salvador FJ, Gimeno J, Bracho G. A new methodology for correcting the signal cumulative phenomenon on injection rate measurements. Exp Tech 2008;15:46–9.

14. Coppo M., Dongiovanni C., Experimental Validation of a Common-Rail Injector Model in the Whole Operation Field, ASME J. of Engineering for Gas Turbines and Power, Vol 129, pp.596 – 608. 2007.

15. Chung, NH., Oh, BH., Sunwoo, MH. Modelling and injection rate estimation of common-rail injectors for direct-injection diesel engines. Proc Inst Mech Eng D, J Automob Eng. Vol. 222, pp. 1089–101. 2008.

16. Payri, R., Tormos, B., Salvador, F.J., Plazas, A.H. Using one-dimensional modelling codes to analyse the influence of diesel nozzle geometry on injection rate characteristics. Int J Vehicle Des. Vol. 38, pp. 58–78. 2005.

17. Catania, A. E., Ferrari, A., Manno, M., Spessa, E., "Termal Effect Simulation in High-Pressure Injection System Transient Flows," SAE Paper No. 2004-01-0532, 2004.

18. Payri, R., Salvador, F.J., Gimeno, J., García, A. Flow regime effects over non-cavitating diesel injection nozzles. Proc. IMechE Vol. 226 Part D: J. Automobile Engineering. (2011)

19. Payri, R., Gimeno, J., Venegas, O., Plazas, A.H. "Effect of partial needle lift on the nozzle flow in diesel fuel injectors". SAE Paper 2011-9116, 2011.

20. Plazas, A. Modelado unidimensional de inyectores common-rail diesel. PhD Thesis. UPV. 2005.

21. K. KARIMI, "Characterization of Multiple-Injection Diesel Sprays at Elevated Pressures and Temperatures", Ph.D. Thesis, University of Brighton, May 2007

22. LMS, "Hydraulic Library Rev 11: User's guide", 2011

23. K. AHLIN, "Modelling of pressure waves in the Common Rail Diesel Injection System", Master thesis, 2000

24. Gauthier, C., Sename, O., Dugard, L. and Meissonnier, G. Modelling of a diesel engine common rail injection system. Proceedings of the 16th IFAC World Congress, 2005. Vol.16, Part 1. 2005. Doi: 10.3182/20050703-6-CZ-1902.01919

25. Lopes, A., Talavera-Prieto, M., Ferreira, A., Santos, J., Santos, M., Portugal, A. Speed of sound in pure fatty acid methyl esters and biodiesel fuels. Fuel, vol. 116, p. 242–254, 2014.

26. R. Payri et al., "The effect of temperature and pressure on thermodynamic properties of diesel and biodiesel fuels" in Fuel Vol. 90, p. 1172-1180, 2011.

27. Tribotte, P., Ravet, F., Dugue, V., Obernesser, P., *et al.*, "Two Strokes Diesel Engine - Promising Solution to Reduce Co2 Emissions." *Procedia - Social and Behavioral Sciences* 48):2295-2314, 2012, doi: 10.1016/j.sbspro.2012.06.1202.

28. Pohorelsky, L., Brynych, P., Macek, J., Vallaude, P.-Y., et al., "Air System Conception for a Downsized Two-Stroke Diesel Engine," SAE Technical Paper 2012-01-0831, 2012, doi: 10.4271/2012-01-0831.

29. Benajes, J., Molina, S., Novella, R., and De Lima, D., "Implementation of the Partially Premixed Combustion Concept in a 2-Stroke Hsdi Diesel Engine Fueled with Gasoline." *Appl. Energy* 122(0):94-111, 2014

30. d'Ambrosio, S.; Ferrari, A. Diesel Injector Coking: Optical-Chemical Analysis of Deposits and Influence on Injected Flow-Rate, Fuel Spray and Engine Performance, Journal of engineering for gas turbines and power-transactions of the asme, Vol 134 (6), DI 10.1115/1.4005991, 2012

Contact Information

Dr. Raúl Payri, rpayri@mot.upv.es

CMT-Motores Térmicos, Universitat Politecnica de Valencia

Acknowledgments

Definitions/Abbreviations

A_{line}	Geometrical cross section of the line
A_o	Geometrical cross section of the holes
B	Bulk Modulus
c	speed of sound
C	Generic definition for coefficients in parametric equations
C_d	Discharge coefficient
CAD	Crank angle degrees
D_o	Outlet hole diameter
DOI	Duration of injection
DT	Dwell Time
EOE	End of Energizing
ET	Energizing Time
$\dot{m}$	Mass Flow rate
P	Pressure
P_b	Back Pressure
P_r	Rail Pressure
Q_{pump}	Volumetric flow of the pump
$Q_{regulator}$	Volumetric flow of the regulator
ROI	Rate of Injection
SOE	Start of Energizing
SOI	Start of injection
T	Temperature

u	Velocity
u_B	Bernoulli theoretical velocity
$W(t)$	Wave function
α	Opening slope
β	Closing slope
ρ_f	Liquid fuel density

APPENDIX 1
Adaptation to used nozzles (blockage coefficient)

Sometimes the injector units lost their efficiency through the time in function of the operating hours. Indeed, when an injector is used during a certain time, the injector does not have the same rate of injection than it had when it was new. The symptom is perceived as a loss of the maximum of the flow rate and a longer injection. For instance, in Figure 22, there is a comparison between two analogous injectors, a new injector and one which is used, the test has been made with a rail pressure of 1.500 bar, a back pressure of 40 bars and an energizing time of 1 ms. This problem is due to the deposit which accumulates into the nozzle of the injectors [30]. That is why the maximum is smaller as there is more loss of velocity which results in a discharge coefficient smaller, as the internal flow is affected, the time for the pressure in the control valve to get back to the rail pressure is greater and that explains the longer injection duration.
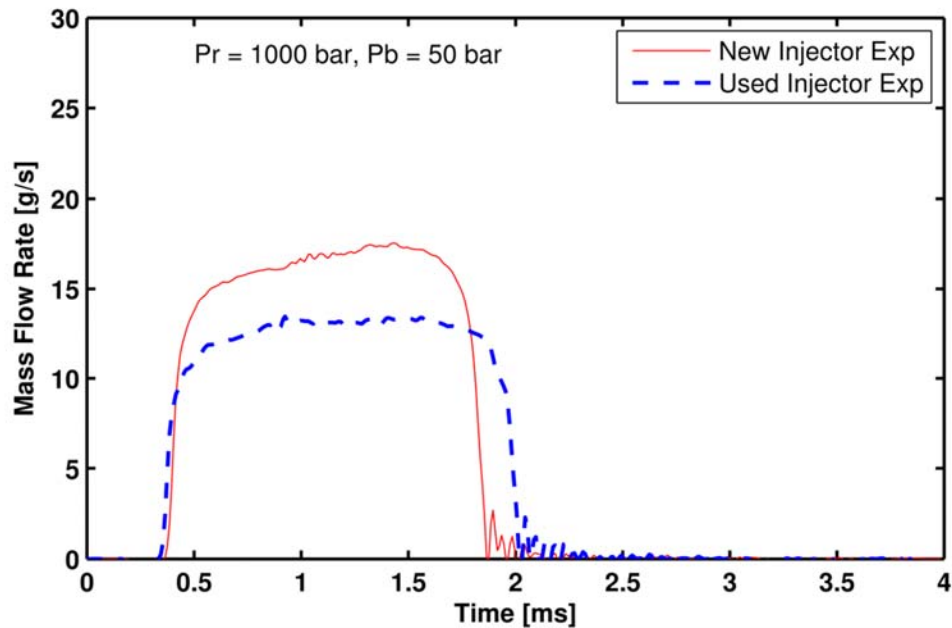
Figure 22. Experimental comparison between new and used injectors

It seems unthinkable to have to test again the used injectors to find the coefficients to be able to model it, besides the phenomenon will be more visible in function of the operating hours. The idea is to readjust the model created for the new injectors to adapt it to the used ones.

The solution has been found with the pressure data indeed the drop of pressure into the common rail system indicates the sign of the beginning and the end of the injection. So the procedure is to find with the pressure data, the real injection duration to correct the problem of the DOI, for the maximum once the injection duration is found the model is created with the good DOI to compare the total mass of the model with the real mass.

This will be done for few injections in order to find right coefficients which could be used for the other tests. The study is decomposed in four main steps:

- Find the duration of the pressure drop from the experimental data: $DOI_{Pressure}$
- Find the equation between these times and the real injection duration
- Find the correlation for the injection duration between the new and old injectors
- Find the factor to adjust the maximum of the flow rate

To find this time, a non-dimensional number is used that is described in the Equation (22)

$$\pi_1 = \frac{P(t) - P_o}{max(P(t) - P_o)} \qquad \textbf{(22)}$$

The equation between the duration of the pressure drop and the injection duration is found with the experimental data of the new injector, this equation is supposed to be linear. However, a correction with the rail pressure and the energizing time will improve the results as shown in Equation (23).

$$DOI = k1_{ID} + k2_{ID} DOI_{pressure} + k3_{ID} ET + k4_{ID} P_r \qquad \textbf{(23)}$$

Once, this equation is found, the used injectors are implemented in order to compare its injection duration with a new one. As shown in the Figure 23, there is a linear correlation between the two injection durations. So, the injection model will just need two coefficients to adjust the duration of the injections. For the efficiency, the real total mass and the one found with the injection model are compared to find the corrective factor which is simply the quotient of these masses.
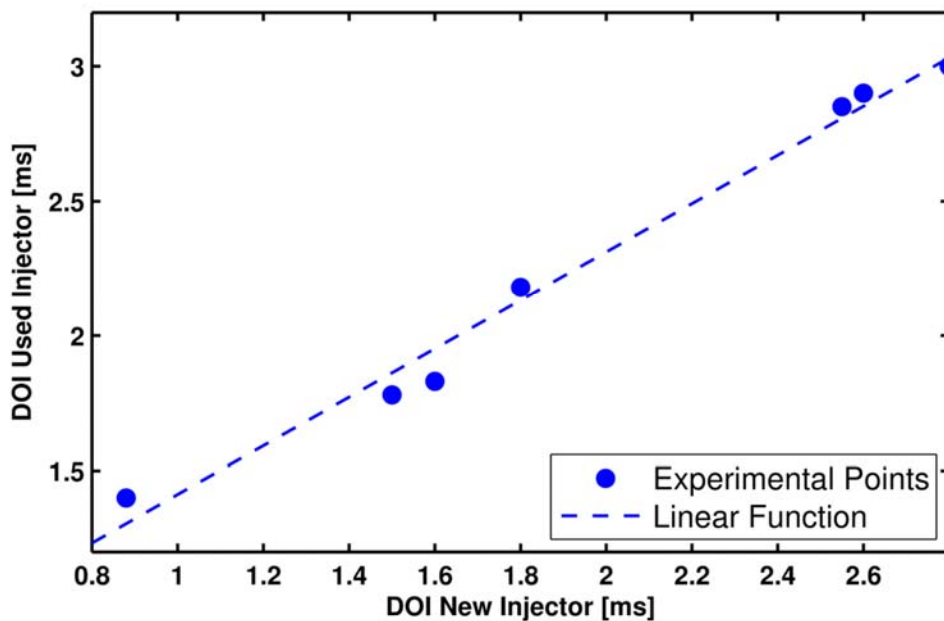

Figure 23. Injection duration Correlation between the new and the old samples

Once the function has found all the coefficients, it returns the difference between the new and the old injections and the impact on the mass. Figure 24 shows the mass flow rate of a used injector and the model results with the two criteria used and new one.
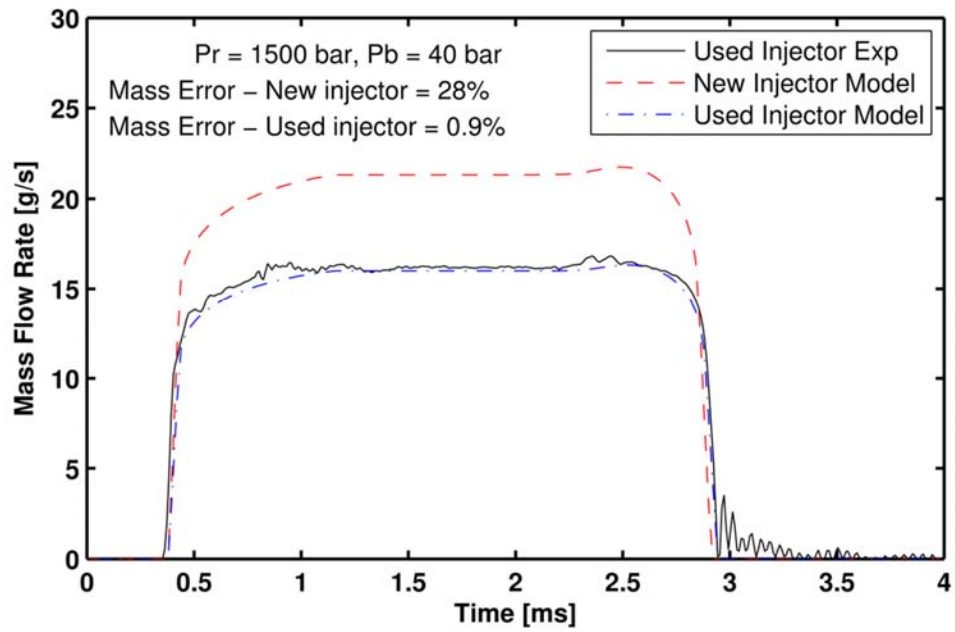
Figure 24. Injection comparison of the used injector data and the models